

# Semaphorin 3A-modified adipose-derived stem cell sheet may improve osseointegration in a type 2 diabetes mellitus rat model

KAIXIU FANG<sup>1\*</sup>, WEN SONG<sup>2\*</sup>, LIFENG WANG<sup>1</sup>, XIAORU XU<sup>1</sup>, NAIWEN TAN<sup>1</sup>,  
SIJIA ZHANG<sup>1</sup>, HONGBO WEI<sup>1</sup> and YINGLIANG SONG<sup>1</sup>

Departments of <sup>1</sup>Oral Implants and <sup>2</sup>Prosthodontics, School of Stomatology,  
State Key Laboratory of Military Stomatology, Fourth Military Medical University, Xi'an, Shaanxi 710032, P.R. China

Received August 25, 2015; Accepted July 4, 2016

DOI: 10.3892/mmr.2016.5568

**Abstract.** Although titanium (Ti) implants are considered to be an optimal choice for the replacement of missing teeth, it remains difficult to obtain sufficient osseointegration in patients with type 2 diabetes mellitus (T2DM). The present study aimed to investigate whether adipose-derived stem cells (ASCs) may be used to improve Ti implant osseointegration in T2DM conditions with the addition of semaphorin 3A (Sema3A), a recently identified osteoprotective protein. Cell morphology was observed using a scanning electron microscope. Cell proliferation was determined using Cell Counting Kit-8. Osteogenic differentiation was confirmed by the staining of alkaline phosphatase, collagen secretion and calcium deposition. An *in vivo* evaluation was performed in the T2DM rat model, which was induced by a high-fat diet and a low-dose streptozotocin intraperitoneal injection. A Sema3A-modified ASC sheet was wrapped around the Ti implant, which was subsequently inserted into the tibia. The rats were then exposed to Sema3A stimulation. The morphology and proliferation ability of ASCs remained unchanged; however, their osteogenic differentiation ability was increased. Micro-computed tomography scanning and histological observations confirmed that formation of new bone was improved with the use of the Sema3A-modified ASCs sheet. The present study indicated that the Sema3A-modified ASCs sheet may be used to improve osseointegration under T2DM conditions.

## Introduction

Titanium (Ti) implants are considered to be the optimal material for teeth replacements and orthopedic devices (1). However, osseointegration of Ti implants remain a challenge in type 2 diabetes mellitus (T2DM) patients. With economic growth and an aging population, the T2DM patient population is increasing rapidly; therefore, there is a high demand for improving osseointegration in T2DM.

Improvement of osseointegration in patients with T2DM has been widely investigated. A previous study reported that the systematic administration of vitamin D3 and insulin improves Ti osseointegration in diabetes mellitus rats (2). Local delivery of basic fibroblast growth factor may also enhance the osseointegration of implants (3). However, the drug delivery method (systematic or local) appears unimportant, as certain drugs work solely in a non-specific manner around the Ti implant, lack targeted intervention and may result in unknown side effects. It is considered that hyperglycemia in T2DM has a negative influence on the differentiation of bone marrow stromal cells (BMSCs) and thus results in deficiencies of these cells during osseointegration (4,5). The introduction of exogenous healthy stem cells into the implant cavity may alleviate this problem. A stem cell sheet consists of numerous cells and bioactive growth factors. In addition, the stem cell sheet is semi-differentiated in order to allow for more effective osseointegration by providing a pre-organized microenvironment for bone formation (6,7). A previous study used BMSCs for this purpose and prepared cell-implant complexes to improve osseointegration in a T2DM model (6). However, the collection of BMSCs requires complex procedures; therefore, the possible application of this treatment is limited by the ability to source BMSCs (8,9). Adipose-derived mesenchymal stem cells (ASCs) are considered as an attractive candidate to replace BMSCs in various areas, including bone tissue regeneration due to their abundant availability and clear expansion capacity (10-13). Therefore, it is possible that an ASCs sheet-wrapped Ti implant may promote osseointegration in a T2DM model. Previous studies have determined that the bone matrix mineralization and calcium deposition abilities of ASCs are weaker compared with BMSCs (14,15). Therefore, it is necessary to further investigate the osteogenic ability of ASCs prior to implantation.

---

*Correspondence to:* Professor Yingliang Song or Dr Hongbo Wei, Department of Oral Implants, School of Stomatology, State Key Laboratory of Military Stomatology, Fourth Military Medical University, 145 West Changle Road, Xi'an, Shaanxi 710032, P.R. China

E-mail: songyingliang@yahoo.com

E-mail: weihongbo101@126.com

\*Contributed equally

**Keywords:** diabetes, implantology, osseointegration, adipose-derived stem cells, semaphorin 3A

Bone homeostasis requires a balance between bone formation and resorption, which is crucial for bone metabolism (16). Certain drugs are able to promote bone formation (17), however, they may also activate bone resorption (18) as a result of dysfunctional bone homeostasis. Semaphorin 3A (Sema3A) was the first member to be identified from the large semaphorin family and has been determined to be a novel osteoprotective protein (19,20). This protein is able to affect osteogenic promotion and bone resorption inhibition (19). Therefore, Sema3A may be effective for use in ASC modification.

The present study assessed the osteogenic capacity of ASCs *in vitro* by Sema3A modification. The constructed ASC sheet was modified by Sema3A prior to being wrapped around a Ti implant and inserted into a T2DM rat to evaluate the osseointegration under T2DM conditions.

## Materials and methods

**Cell isolation and culture.** A total of 20 adult male Sprague-Dawley rats (age, 6-8 weeks; weight, 150-200 g) were obtained from the Laboratory Animal Center of Fourth Military Medical University (FMMU; Xi'an, China). They were maintained under a 12-h light/dark cycle with access to a normal diet, at 18-26°C and a humidity of 30-70%. The animal experiment procedures were approved by the Animal Welfare Committee of the FMMU. Primary rat ASCs were isolated as previously described (21). Briefly, the subcutaneous adipose tissue was harvested from the inguinal fat pad and washed with phosphate-buffered saline (PBS). The tissue was finely minced into pieces and digested at 37°C with 0.1% type I collagenase (MP Biomedicals LLC, Santa Ana, CA, USA) for 40 min. The digestion was terminated by growth medium (GM) composed of Dulbecco's modified Eagle's medium, Ham's F12 nutrient mixture, 10% fetal bovine serum and 1% penicillin/streptomycin (all from Hyclone; GE Healthcare, Logan, UT, USA). The digested product was centrifuged at 120 x g for 5 min at room temperature and the pellet was resuspended in GM for culturing. Cells at passage 3-6 were used for the further investigation. In order to perform the osteogenic differentiation in the presence of Sema3A, conditioned medium (CM) was prepared by supplementing 10 mM  $\beta$ -glycerophosphate, 50  $\mu$ g/ml ascorbic acid, 10 nM dexamethasone (all from MP Biomedicals LLC) and different concentrations (0, 0.25, 0.5 and 1.0  $\mu$ g/ml) of Sema3A (PeproTech, Inc., Rocky Hill, NJ, USA) into the GM. The treatment groups were then named ASCs, ASCs-0.25, ASCs-0.5 and ASCs-1.0.

**Morphological observations.** The ASCs were seeded onto coverslips (5x5 mm) at a density of  $2.0 \times 10^4$  cells/well in a 24-well plate and incubated for 24 h. Subsequently, the samples were fixed in 2.5% glutaraldehyde and dehydrated gradually in ethanol (from 30-100%). The sample was further dried under critical point conditions and sputter coated with platinum. Observations were then performed using a scanning electron microscope (SEM; S-4800; Hitachi, Ltd., Tokyo, Japan; magnification, x200).

**Cell proliferation analysis.** The ASCs were seeded in 96-well plates at a density of  $1.0 \times 10^4$  cells/well. Cell viability was

continuously monitored each day using Cell Counting Kit-8 (CCK-8; MP Biomedicals LLC) according to the manufacturer's protocol. Briefly, 10  $\mu$ l CCK-8 solution was gently mixed with phenol red-free medium in each well and incubated for 3 h at 37°C. The medium was then transferred into a new 96-well plate, and the absorbance was detected at 450 nm by a microplate reader (Epoch; BioTek Instruments, Inc., Winooski, VT, USA).

**Reverse transcription-quantitative polymerase chain reaction (RT-qPCR).** The ASCs were seeded in 24-well plates at a density of  $2.0 \times 10^4$  cells/well. Subsequent to expansion for 3 days in GM, the cells were induced with CM. Following 3 and 7 day induction periods, total RNA was isolated using TRIzol reagent (Invitrogen; Thermo Fisher Scientific, Inc., Waltham, MA, USA) and 1  $\mu$ g total RNA was reverse transcribed to complementary DNA (cDNA) using PrimeScript RT reagent kit (Takara Biotechnology Co., Ltd., Dalian, China). Osteogenesis-associated genes, including alkaline phosphatase (ALP) and collagen type I  $\alpha 1$  (COL1A1), were amplified using a SYBR Premix Ex Taq II RT-PCR kit (Takara Biotechnology Co., Ltd.). A 10  $\mu$ l system containing 5  $\mu$ l SYBR Premix, 1  $\mu$ l forward primer, 1  $\mu$ l reverse primer and 3  $\mu$ l cDNA was used. The thermocycling conditions were 40 cycles of 95°C for 15 sec and 60°C for 30 sec. The PCR was analyzed using CFX Manager software version 3.1 (Bio-Rad Laboratories, Inc., Hercules, CA, USA). The primers used are presented in Table I and were as previously described (22). The mRNA expression was calculated based on the Cq value (23), and glyceraldehyde 3-phosphate dehydrogenase (GAPDH) was used as the endogenous reference.

**Osteogenesis staining.** ALP production, collagen secretion and extracellular matrix (ECM) mineralization were visualized using 5-bromo-4-chloro-3-indolyl-phosphate (BCIP)/nitro blue tetrazolium (NBT) alkaline phosphatase, Sirius red and Alizarin red S (all from Leagene Biotech Co., Ltd., Beijing, China) staining. Following induction in CM for 7, 14 and 21 days, the cells were fixed in 2.5% glutaraldehyde for 15 min at room temperature. Next, the specimens were stained by BCIP/NBT alkaline phosphatase solution, Sirius red and Alizarin red according to the manufacturer's protocol. The cells were rinsed with PBS in order to remove any excess dye and images were captured using a stereo microscope (Leica Microsystems, Inc., Buffalo Grove, IL, USA; magnification, x20).

**Cell sheet construction and surgical implantation.** The construction of the ASC sheets was performed as previously described (24). Briefly, cells were seeded into 6-well plates at a density of  $3.0 \times 10^5$  cells/well and allowed to expand for 24 h to reach 100% confluence. Following *in vitro* observation, it was determined that Sema3A at the highest concentration (1.0  $\mu$ g/ml) and ascorbic acid (50  $\mu$ g/ml) should be added into the GM to perform the cell sheet engineering. The control group was induced without Sema3A. The cell sheet was formulated after 1 week and was allowed to shrink instantly subsequent to detachment of the forceps. The sheet wrapped closely around the implant (L=5 mm; D=1.5 mm; provided by Northwest Institute for Nonferrous Metal Research, Xi'an, China).

Table I. Primer sequences used for reverse transcription-quantitative polymerase chain reaction.

Gene	Forward (5'-3')	Reverse (5'-3')
<i>ALP</i>	CCTTG TAGCCAGGCCATTG	GGACCATTCCCACGTCTTCAC
<i>COL1A1</i>	CCTACAGCACGCTTGTGGAT	ATTGGGATGGAGGGAGTTTA
<i>GAPDH</i>	CAAGTTCAACGGCACAGTCA	CCATTTGATGTTAGCGGGAT

*ALP*, alkaline phosphatase; *COL1A1*, collagen type I  $\alpha 1$ ; *GAPDH*, glyceraldehyde 3-phosphate dehydrogenase.

A high-fat diet and a low-dose (30 mg/kg) streptozotocin (MP Biomedicals LLC) intraperitoneal injection was administered to induce T2DM as described previously (6). Animals were anesthetized by an intra-abdominal injection of a pentobarbital sodium solution (Sigma-Aldrich, St. Louis, MO, USA) at a dose of 50 mg/kg. Following shaving and sterilization, the implant cavity (D=1.8 mm) was prepared at approximately 7 mm below the knee joint using a twist drill. Subsequently, the cell sheet-embedded implant was inserted into the cavity. A post-operative antibiotic treatment, based on body weight, was injected once a day for seven days.

**Micro-computed tomography (CT) scanning and histological evaluation.** The healing process was 4-8 weeks, then the rats were subsequently sacrificed by intraperitoneal injection of overdose (>100 mg/kg) of pentobarbital sodium solution and the specimens were scanned by micro-CT (scanning resolution, 50  $\mu\text{m}$ ) in order to determine alterations in the peri-implant tissue. The region of interest (ROI), including the trabecular compartment surrounding the implant, was defined as a ring with a radius of 1.25 mm from the implant surface. In the three-dimensional level, the Hounsfield unit of this newly formed bone area was determined using the Inveon Research Workplace software package, version 2.2.0 (Siemens Healthcare GmbH, Erlangen, Germany). The trabecular thickness, trabecular number and bone volume ratio were determined and recorded. The tibia tissue was isolated and fixed in 10% formalin (pH=6.7) at 4°C. The samples were dehydrated in a graded ascending series of ethanol solutions (70-100%), infiltrated and embedded in methyl methacrylate. Serial sections (150  $\mu\text{m}$ ) along the implant axis were obtained using a high-speed precision microtome (SP1600; Leica Microsystems, Inc.). All sections were ground and polished to a thickness of 35  $\mu\text{m}$ . The sections were surface-stained using a Van Gieson solution and observed using an optical microscope (Olympus Corporation, Tokyo, Japan).

**Statistical analysis.** The quantitative data were expressed as the mean  $\pm$  standard deviation. A one-way analysis of variance followed by a Student-Newman-Keuls post-hoc test was used to compare the means.  $P < 0.05$  was considered to indicate a statistically significant difference.

## Results

**Cell morphology and proliferation remains unchanged with *Sema3A* treatment.** The morphology and proliferation of ASCs under different concentrations of *Sema3A* were observed

(Fig. 1). The cells spread widely with abundant cell-cell connections and no significant differences were identified under SEM observation (Fig. 1A). Additionally, no significant difference in cell proliferation was identified subsequent to treatment with various concentrations of *Sema3A* (Fig. 1B).

***Sema3A* upregulates expression levels of osteogenic-associated genes.** The RT-qPCR analysis determined that *ALP* and *COL1A1* mRNA expression levels were significantly upregulated, mostly in line with the increase of *Sema3A* concentration ( $P < 0.05$ ; Fig. 2). Specifically, the mRNA levels of *ALP* and *COL1A1* increased by 5-fold and 7-fold, respectively, following treatment with *Sema3A* from 0.25 to 1.0  $\mu\text{g}/\text{ml}$  at day 3 (Fig. 2A). At day 7, the mRNA levels increased significantly when compared with the control ASCs group by 7-fold and 5-fold, respectively, in the *ALP* and *COL1A1* groups ( $P < 0.05$ ; Fig. 2B).

***Osteogenesis staining is altered by *Sema3A*.*** The osteogenic differentiation was further analyzed by staining for ALP production, collagen secretion and ECM mineralization using BCIP/NBT, Sirius red and Alizarin red staining, respectively. In agreement with the gene expression data, the ALP production and collagen secretion were observed to be greater with the increase of *Sema3A* concentration (Fig. 3). No differences between the treatment groups were identified from the ECM mineralization of the samples, however this may be due to insufficient induction time.

***Osseointegration is greater in rats implanted with *Sema3A* ASC sheets.*** To confirm that *Sema3A* may improve osseointegration *in vivo*, ASC sheets were produced and modified with *Sema3A* in order to coat Ti implants. The formation of new bone around the implant was examined by micro-CT scanning (Fig. 4). The *Sema3A*-modified ASC sheets had formulated more new bone (green section) around the implant (red section), 4 weeks and 8 weeks subsequent to insertion (Fig. 4A). The quantitative analysis of the ROI demonstrated that the new bone volume and number (4 weeks) and the new bone volume, thickness and number (8 weeks) were significantly greater in the rats implanted with the *Sema3A*-modified ASC sheet compared with the ASCs only sheet ( $P < 0.05$ ; Fig. 4B-D).

***Bone formation is increased in rats with *Sema3A*-modified ASC sheets compared with ASC-only rats.*** In the ASC sheet-only group, 4 weeks after implantation, the new bone formation observed was thin compared with the intermittent

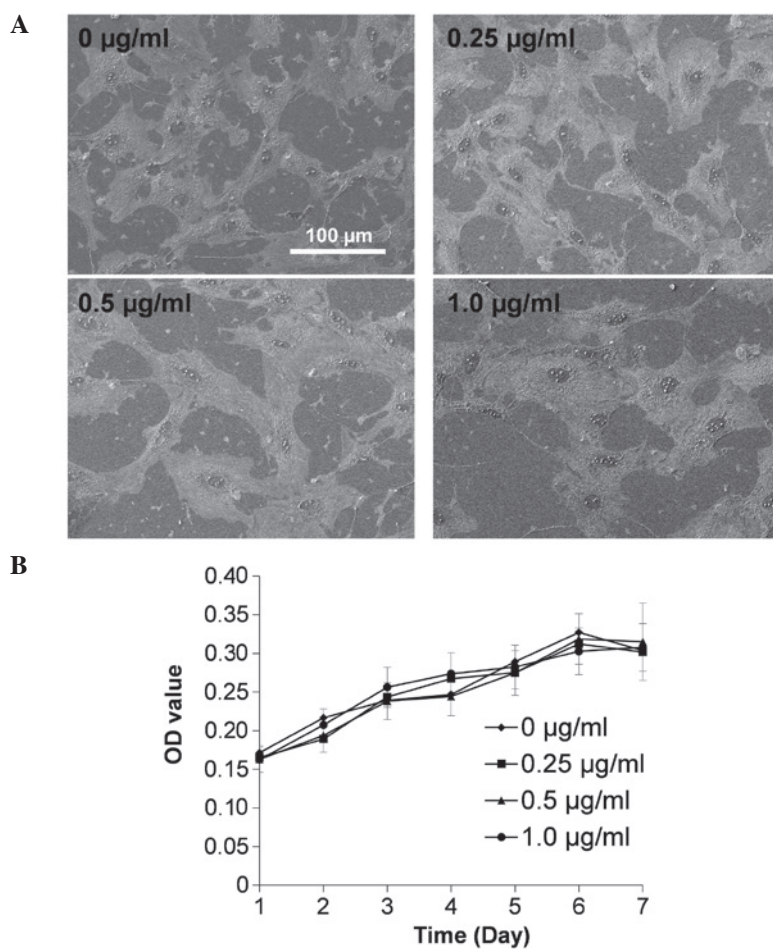


Figure 1. Morphology and proliferation rate of adipose-derived stem cells subsequent to exposure to different semaphorin 3A concentrations remained unchanged. (A) Cells were cultured for 24 h and observed under scanning electron microscope. (B) Cell viability was detected by Cell Counting Kit-8 continuously for 7 days and was consistent across all treatment groups. OD, optical density.

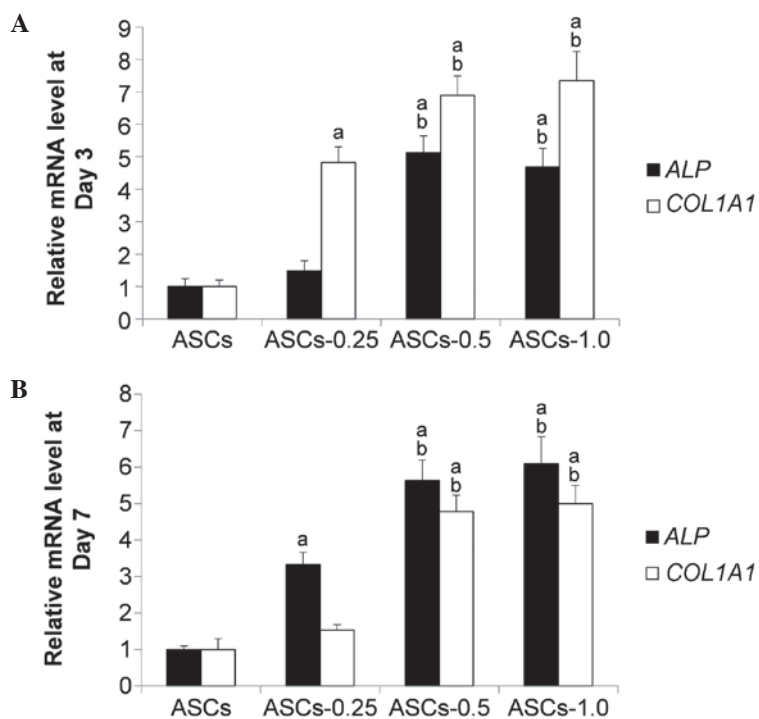


Figure 2. Reverse transcription-quantitative polymerase chain reaction analysis to determine mRNA levels of genes associated with osteogenic differentiation (*ALP* and *COL1A1*). The mRNA levels were observed following induction in osteogenic medium containing different semaphorin 3A concentrations after (A) 3 and (B) 7 days. \* $P < 0.05$  vs. ASCs. <sup>a</sup> $P < 0.05$  vs. ASCs-0.25. ASCs, adipose-derived stem cells; *ALP*, alkaline phosphatase; *COL1A1*, collagen type I  $\alpha 1$ .

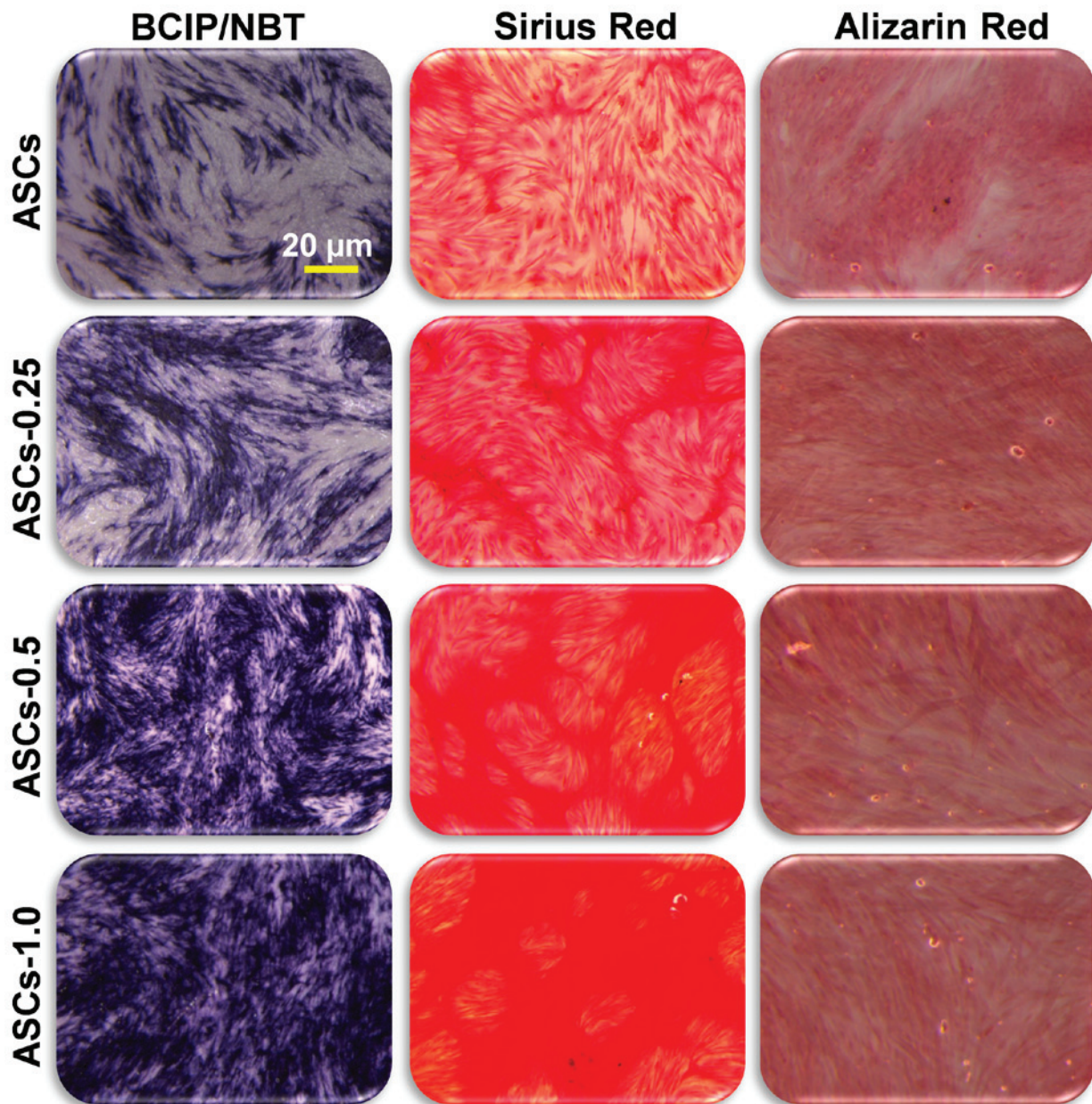


Figure 3. Alkaline phosphatase production, collagen secretion and extracellular matrix mineralization in ASCs were determined using BCIP/NBT, Sirius red and Alizarin red staining, following induction of cells in osteogenic medium containing different concentrations of semaphorin 3A for 7, 14 and 21 days. ASCs, adipose-derived stem cells; BCIP/NBT, 5-bromo-4-chloro-3-indolyl-phosphate/nitro blue tetrazolium.

but thicker new bone formation around the implant surface observed in the Sema3A-modified ASCs sheet group (Fig. 5). At 8 weeks post-implantation, fragmented new bone formation was observed in the ASC sheet-only group, whereas continuous and thick new bone formation was evident in the Sema3A-modified ASC sheet group (Fig. 5).

### Discussion

The proportion of the human population diagnosed with T2DM has increased rapidly worldwide, resulting in a clear health problem. Bone tissue is primarily damaged by the high glucose levels, which lead to the suppression of differentiation in osteoblastic lineage cells (25). To improve osseointegration in patients with T2DM, the current study

introduced exogenous stem cells into the Ti implant periphery. The osteogenic capacity of ASCs was significantly increased with increases in Sema3A concentration. Therefore, ASCs are suggested to be suitable for bone engineering following Sema3A modification.

According to a previous study (19), the binding of Sema3A to neuropilin-1 may stimulate osteoblast and inhibit adipocyte differentiation via the canonical Wnt/ $\beta$ -catenin signaling pathway. However, whether the same molecular mechanism is active in ASCs remains to be elucidated. It is of note that an association between Sema3A and mesenchymal stem cells has been demonstrated. BMSCs have been identified to express Sema3A in order to regulate T-cell immunosuppression (26). The stimuli of Sema3A has been reported to induce mesenchymal stem cell-like properties in human periodontal

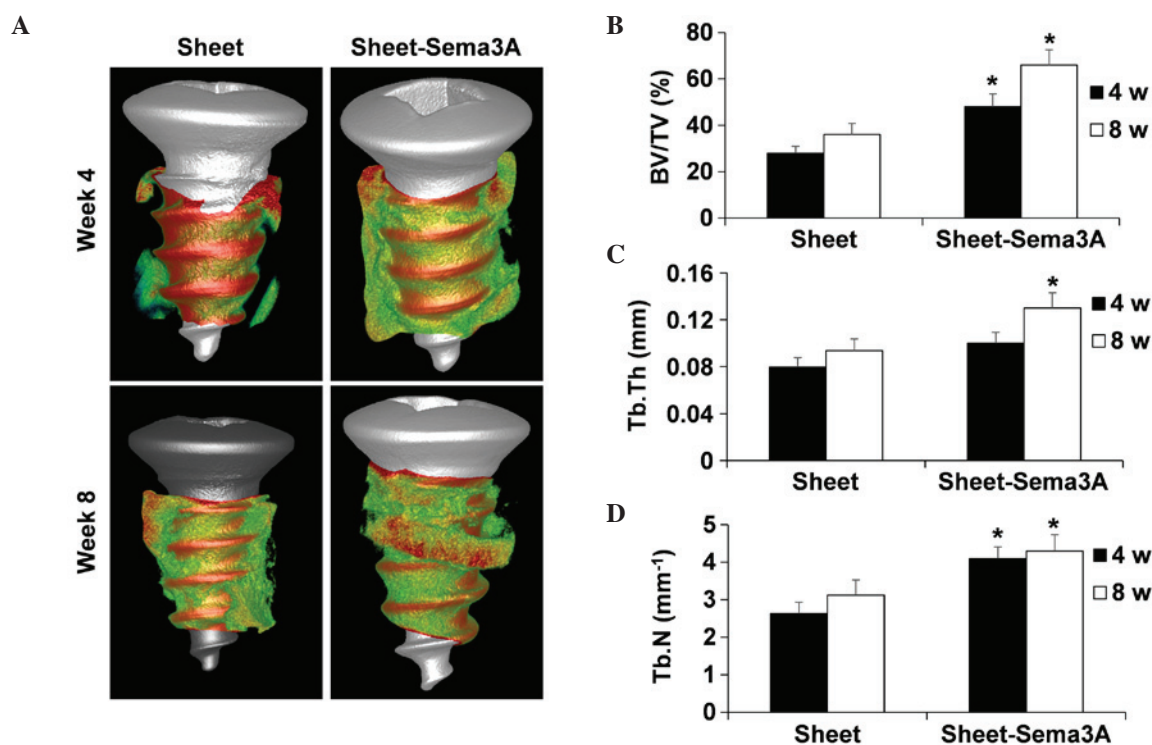


Figure 4. Micro-computed tomography evaluation after 4 and 8 weeks of healing. The ROI was defined as a ring with a radius of 1.25 mm from the implant surface. (A) 3D reconstruction of new bone formation surrounding the peri-implant. The red area indicates the titanium implant and the green area represents new bone formation within the ROI. (B) BV/TV, (C) Tb.Th and (D) Tb.N were also calculated. \* $P < 0.05$  vs. sheet-only group. Sema3A, semaphorin 3A; BV/TV, bone volume ratio; Tb.Th, trabecular thickness; Tb.N, trabecular number; ROI, region of interest.

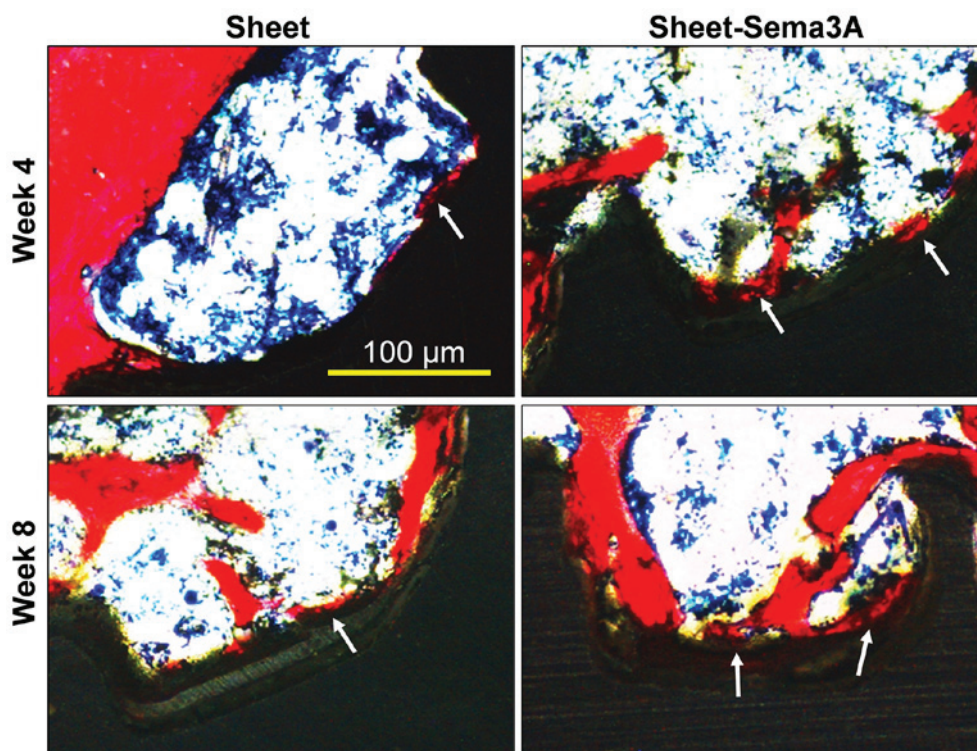


Figure 5. Histological analysis was performed by ultra-rigidity slicing followed by Van Gieson staining after 4 and 8 weeks of healing. The black area is the titanium implant and red area depicts bone tissue. The white arrows indicate the new bone formation on the implant surface. Sema3A, semaphorin 3A.

ligament cells (27). Therefore, although the exact osteogenesis mechanism in ASCs remains unclear, it may be inferred that Sema3A and ASCs interact closely.

The morphology of stem cells may allow for determination of differentiation status. The spindle fibroblast-like shape indicates a low differentiation status, whereas the polygonal

osteoblast-like shape indicates potential osteogenic differentiation (28). However, the present study has determined that all cells spread widely without clear morphological alterations subsequent to *Sema3A* treatment. This may be due to short incubation time; therefore the cells were unable to exhibit a morphological difference. In addition, it is possible that cell shape may be predominantly defined by substrate topography. Although *Sema3A* has been associated with cytoskeleton reorganization (29), the present study did not identify any alterations in the morphology of ASCs treated with *Sema3A*. Therefore, when the cells are grown on a glass surface, the ultra-smooth topography may give cells the opportunity to spread freely in all directions without obstacles. Proliferation is primarily recognized as the opposite of differentiation, as differentiated cells have demonstrated low proliferation and mitotic cells are not terminally differentiated (30). However, a recent study identified that proliferation and differentiation are two distinct translational programs (31). The current study confirmed that *Sema3A* may improve the osteogenic ability of ASCs without inducing their proliferation.

In order to determine the formation of new bone *in vivo*, micro-CT scanning and super-rigidity slicing were performed. Similar to the results of the *in vitro* experiments, the *Sema3A* pre-treated ASC sheet significantly improved the formation of new bone around the Ti implant. It is of note that *Sema3A* is only used during the ASC sheet formulation *in vitro*, while the *in vivo* bone formation enhancement occurs several weeks later. Therefore, the effect of *Sema3A* is evident in the differentiation process of the ASCs in the sheet long after its administration. A previous study observed that the osteogenic promotion effect of *Sema3A* is effective at the initial stage (27). Therefore, *Sema3A* is convenient to use in conjunction with Ti implants. There is a variety of bioactive molecules that may promote bone metabolism and previous studies have aimed to establish a sustained drug delivery system to acquire a prolonged effect. *Sema3A* allows for treatment at the initial stage and avoids the problems surrounding long-term delivery. Another important advantage of the current study is that the systematic infusion of ASCs has been validated as a novel therapy for T2DM (32). *Sema3A*-modified ASCs may be a reliable choice for improving osseointegration in T2DM patients.

The present study demonstrated that *Sema3A* may significantly improve the osteogenesis ability of the ASC sheet and may be able to facilitate osseointegration under T2DM conditions.

### Acknowledgements

The present study was supported by National Natural Science Foundation of China (grant nos. 81170984, 81470775 and 81300918). The manuscript was been revised by the Elsevier English Language Service. The authors would like to thank the Department of Oral and Maxillofacial Surgery, School of Stomatology, Fourth Military Medical University (Xi'an, China) for the technical assistance.

### References

- Pjetursson BE, Brägger U, Lang NP and Zwahlen M: Comparison of survival and complication rates of tooth-supported fixed dental prostheses (FDPs) and implant-supported FDPs and single crowns (SCs). *Clin Oral Implants Res* 18 (Suppl 3): 97-113, 2007.
- Wu YY, Yu T, Yang XY, Li F, Ma L, Yang Y, Liu XG, Wang YY and Gong P: Vitamin D3 and insulin combined treatment promotes titanium implant osseointegration in diabetes mellitus rats. *Bone* 52: 1-8, 2013.
- Zou GK, Song YL, Zhou W, Yu M, Liang LH, Sun DC, Li DH, Deng ZX and Zhu WZ: Effects of local delivery of bFGF from PLGA microspheres on osseointegration around implants in diabetic rats. *Oral Surg Oral Med Oral Pathol Oral Radio* 114: 284-289, 2012.
- Mellado-Valero A, Ferrer García JC, Herrera Ballester A and Labaig Rueda C: Effects of diabetes on the osseointegration of dental implants. *Med Oral Patol Oral Cir Bucal* 12: E38-E43, 2007.
- Gopalakrishnan V, Vignesh RC, Arunakaran J, Aruldas MM and Srinivasan N: Effects of glucose and its modulation by insulin and estradiol on BMSC differentiation into osteoblastic lineages. *Biochem Cell Biol* 84: 93-101, 2006.
- Yu M, Zhou W, Song Y, Yu F, Li D, Na S, Zou G, Zhai M and Xie C: Development of mesenchymal stem cell-implant complexes by cultured cells sheet enhances osseointegration in type 2 diabetic rat model. *Bone* 49: 387-394, 2011.
- Yan J, Zhang C, Zhao Y, Cao C, Wu K, Zhao L and Zhang Y: Non-viral oligonucleotide anti-miR-138 delivery to mesenchymal stem cell sheets and the effect on osteogenesis. *Biomaterials* 35: 7734-7749, 2014.
- Auquier P, Macquart-Moulin G, Moatti JP, Blache JL, Novakovitch G, Blaise D, Faucher C, Viens P and Maraninchi D: Comparison of anxiety, pain and discomfort in two procedures of hematopoietic stem cell collection: Leukapheresis and bone marrow harvest. *Bone Marrow Transplant* 16: 541-547, 1995.
- Nishimori M, Yamada Y, Hoshi K, Akiyama Y, Hoshi Y, Morishima Y, Tsuchida M, Fukuhara S and Kodera Y: Health-related quality of life of unrelated bone marrow donors in Japan. *Blood* 99: 1995-2001, 2002.
- Hiwatashi N, Hirano S, Mizuta M, Tateya I, Kanemaru S, Nakamura T and Ito J: Adipose-derived stem cells versus bone marrow-derived stem cells for vocal fold regeneration. *Laryngoscope* 124: E461-E469, 2014.
- Semon JA, Maness C, Zhang X, Sharkey SA, Beuttler MM, Shah FS, Pandey AC, Gimble JM, Zhang S, Scruggs BA, et al: Comparison of human adult stem cells from adipose tissue and bone marrow in the treatment of experimental autoimmune encephalomyelitis. *Stem Cell Res Ther* 5: 2, 2014.
- Lin YC, Grahovac T, Oh SJ, Ieraci M, Rubin JP and Marra KG: Evaluation of a multi-layer adipose-derived stem cell sheet in a full-thickness wound healing model. *Acta Biomater* 9: 5243-5250, 2013.
- Romagnoli C and Brandi ML: Adipose mesenchymal stem cells in the field of bone tissue engineering. *World J Stem Cells* 6: 144-152, 2014.
- Liao HT and Chen CT: Osteogenic potential: Comparison between bone marrow and adipose-derived mesenchymal stem cells. *World J Stem Cells* 6: 288-295, 2014.
- Niemeyer P, Fechner K, Milz S, Richter W, Suedkamp NP, Mehlhorn AT, Pearce S and Kasten P: Comparison of mesenchymal stem cells from bone marrow and adipose tissue for bone regeneration in a critical size defect of the sheep tibia and the influence of platelet-rich plasma. *Biomaterials* 31: 3572-3579, 2010.
- Kini U and Nandeesh BN: Physiology of bone formation, remodeling and metabolism. In: *Radionuclide and Hybrid Bone Imaging*. Fogelman I, Gnanasegaran G and van der Wall H (eds). Springer Berlin Heidelberg, pp29-57, 2012.
- Hodsman AB, Bauer DC, Dempster DW, Dian L, Hanley DA, Harris ST, Kendler DL, McClung MR, Miller PD, Olszanski WP, et al: Parathyroid hormone and teriparatide for the treatment of osteoporosis: A review of the evidence and suggested guidelines for its use. *Endocr Rev* 26: 688-703, 2005.
- Neer RM, Arnaud CD, Zanchetta JR, Prince R, Gaich GA, Reginster JY, Hodsman AB, Eriksen EF, Ish-Shalom S, Genant HK, et al: Effect of parathyroid hormone (1-34) on fractures and bone mineral density in postmenopausal women with osteoporosis. *N Engl J Med* 344: 1434-1441, 2001.
- Hayashi M, Nakashima T, Taniguchi M, Kodama T, Kumanogoh A and Takayanagi H: Osteoprotection by semaphorin 3A. *Nature* 485: 69-74, 2012.
- Fukuda T, Takeda S, Xu R, Ochi H, Sunamura S, Sato T, Shibata S, Yoshida Y, Gu Z, Kimura A, et al: *Sema3A* regulates bone-mass accrual through sensory innervations. *Nature* 497: 490-493, 2013.

21. Pieri F, Lucarelli E, Corinaldesi G, Aldini NN, Fini M, Parrilli A, Dozza B, Donati D and Marchetti C: Dose-dependent effect of adipose-derived adult stem cells on vertical bone regeneration in rabbit calvarium. *Biomaterials* 31: 3527-3535, 2010.
22. Zhang G, Guo B, Wu H, Tang T, Zhang BT, Zheng L, He Y, Yang Z, Pan X, Chow H, *et al*: A delivery system targeting bone formation surfaces to facilitate RNAi-based anabolic therapy. *Nat Med* 18: 307-314, 2012.
23. Livak KJ and Schmittgen TD: Analysis of relative gene expression data using real-time quantitative PCR and the 2<sup>-</sup>(Delta Delta C(T)) method. *Methods* 25: 402-408, 2001.
24. Cerqueira MT, Pirraco RP, Santos TC, Rodrigues DB, Frias AM, Martins AR, Reis RL and Marques AP: Human adipose stem cells cell sheet constructs impact epidermal morphogenesis in full-thickness excisional wounds. *Biomacromolecules* 14: 3997-4008, 2013.
25. Hamann C, Goettsch C, Mettelsiefen J, Henkenjohann V, Rauner M, Hempel U, Bernhardt R, Fratzl-Zelman N, Roschger P, Rammelt S, *et al*: Delayed bone regeneration and low bone mass in a rat model of insulin-resistant type 2 diabetes mellitus is due to impaired osteoblast function. *Am J Physiol Endocrinol Metab* 301: E1220-E1228, 2011.
26. Lepelletier Y, Lecourt S, Renand A, Arnulf B, Vanneaux V, Ferman JP, Menasché P, Domet T, Marolleau JP, Hermine O and Larghero J: Galectin-1 and semaphorin-3A are two soluble factors conferring T-cell immunosuppression to bone marrow mesenchymal stem cell. *Stem Cells Dev* 19: 1075-1079, 2010.
27. Wada N, Maeda H, Hasegawa D, Gronthos S, Bartold PM, Menicanin D, Fujii S, Yoshida S, Tomokiyo A, Monnouchi S and Akamine A: Semaphorin 3A induces mesenchymal-stem-like properties in human periodontal ligament cells. *Stem Cells Dev* 23: 2225-2236, 2014.
28. Zhao L, Liu L, Wu Z, Zhang Y and Chu PK: Effects of micro-pitted/nanotubular titania topographies on bone mesenchymal stem cell osteogenic differentiation. *Biomaterials* 33: 2629-2641, 2012.
29. Nakamura F, Kumeta K, Hida T, Isono T, Nakayama Y, Kuramata-Matsuoka E, Yamashita N, Uchida Y, Ogura K, Gengyo-Ando K, *et al*: Amino- and carboxyl-terminal domains of Filamin-A interact with CRMP1 to mediate Sema3A signalling. *Nat Commun* 5: 5325, 2014.
30. Klochender A, Weinberg-Corem N, Moran M, Swisa A, Pochet N, Savova V, Vikeså J, Van de Peer Y, Brandeis M, Regev A, *et al*: A transgenic mouse marking live replicating cells reveals in vivo transcriptional program of proliferation. *Dev Cell* 23: 681-690, 2012.
31. Gingold H, Tehler D, Christoffersen NR, Nielsen MM, Asmar F, Kooistra SM, Christophersen NS, Christensen LL, Borre M, Sørensen KD, *et al*: A dual program for translation regulation in cellular proliferation and differentiation. *Cell* 158: 1281-1292, 2014.
32. Hu J, Fu Z, Chen Y, Tang N, Wang L, Wang F, Sun R and Yan S: Effects of autologous adipose-derived stem cell infusion on type 2 diabetic rats. *Endocr J* 62: 339-352, 2015.